Great Basin Naturalist 54(4), © 1994, pp. 313–328

GEOSTATISTICAL ANALYSIS OF RESOURCE ISLANDS UNDER *ARTEMISIA TRIDENTATA* IN THE SHRUB-STEPPE

Jonathan J. Halvorson[1], Harvey Bolton, Jr.[2], Jeffrey L. Smith[3], and Richard E. Rossi[2]

Abstract.—Desert plants can influence the pattern of resources in soil resulting in small-scale enriched zones. Although conceptually simple, the shape, size, and orientation of these "resource islands" are difficult to study in detail using conventional sampling regimes. To demonstrate an alternative approach, we sampled soil under and around individual *Artemisia tridentata* (sagebrush), a dominant shrub of cool desert environments, and analyzed the samples with univariate statistics and geostatistics. Univariate statistics revealed that soil variables like total inorganic-N, soluble-C, and microbial biomass-C were distributed with highest mean values within about 25 cm of the plant axis and significantly lower mean values at distances beyond 60 cm. However, such simple analyses restricted our view of resource islands to identically sized, symmetrical accumulations of soil resources under each plant.

Geostatistics provided additional information about spatial characteristics of soil variables. Variography revealed that samples separated by a distance of less than about 70 cm were correlated spatially. Over 75% of the sample variance was attributable to spatial variability. We modeled these spatial relationships and used kriging to predict values for unsampled locations. Resulting maps indicated that magnitude, size, and spatial distribution of soil resource islands vary between individual plants and for different soil properties. Maps, together with cross-variography, further indicate that resource islands under *A. tridentata* are not always distinguishable from the surrounding soil by sharp transition boundaries and may be asymmetrically distributed around the plant axis.

Key words: resource islands, geostatistics, Artemisia tridentata, *nutrient availability, kriging, spatial correlation.*

Recognition that individual plants can significantly affect the local soil environment dates back to at least the middle of the nineteenth century (see Zinke 1962) and has been documented for many plant forms including broadleaf and coniferous trees (Zinke 1962, Everett et al. 1986, Doescher et al. 1987, Belsky et al. 1989), bunch grasses (Hook et al. 1991), herbaceous legumes (Halvorson et al. 1991), and, in particular, desert shrubs (e.g., Fireman and Hayward 1952, Garcia-Moya and McKell 1970, Nishita and Haug 1973, Barth and Klemmedson 1978, Burke 1989, Burke et al. 1989, Virginia and Jarell 1983, Bolton et al. 1990, 1993). Soil associated with plants typically contains greater concentrations of limiting resources (e.g., N, P), contains larger populations of soil microorganisms, and exhibits higher rates of nutrient cycling processes like mineralization (Charley and West 1977, Bolton et al. 1990) and denitrification (Virginia et al. 1982). These small-scale enriched zones, variously termed "fertile islands" (Garner and Steinberger 1989), "isles of fertility" (West 1981, Whitford 1986), "resource islands" (Reynolds et al. 1990), or "ecotessara" (Jenny 1980), are hypothesized to result from several mechanisms (Garner and Steinberger 1989), including litter-fall or stemflow (Zinke 1962), decreased erosion or increased deposition (Coppinger et al. 1991), microclimatological amelioration of the soil (Smith et al. 1987, Pierson and Wight 1991), or inputs of resources via insects, birds, or animals (Davidson and Morton 1984).

Detailed knowledge of the size and internal dynamics of resource islands is important for understanding energy flux, mass transport, and nutrient cycling processes at the scale of the individual plant. Resource islands may also connote a tier in a progressive, hierarchical mosaic of plant and animal habitats, resource distributions, and biogeochemical processes (i.e., patches sensu Kotliar and Wiens 1990). Estimates of the distribution and numbers of resource islands in the landscape may aid in understanding population level processes and can be used to refine regional estimates of

[1]Pacific Northwest Laboratory, Richland, Washington 99352. Direct correspondence to 215 Johnson Hall, Washington State University, Pullman, Washington 99164-6421.
[2]Pacific Northwest Laboratory, Richland, Washington 99352.
[3]Land Management and Water Conservation Research Unit, USDA-ARS, Washington State University, Pullman, Washington 99164.

energy flow and mass transfer. Furthermore, interrelationships of large numbers of individual resource islands may influence ecosystem structure, function, and stability (Reynolds et al. 1990, Schlesinger et al. 1990, Halvorson et al. 1991).

Although conceptually simple, the size, shape, and orientation of resource islands are not easy to evaluate. Previous studies have typically been based on relatively small numbers of samples collected using a binary regime (i.e., samples collected beneath the plant versus samples collected "away" from the plant) or along a transect passing from plant to bare soil. Such an approach cannot be used to provide a detailed spatial analysis of resource concentrations or processes in the soil that are likely to exhibit complex responses to landscape and microsite variations (Burke et al. 1989). Additionally, data collected from different locations (or depths) have often been analyzed using inferential statistics such as ANOVA or *t* tests that assume samples are spatially independent and identically distributed. However, these assumptions may be dubious, if untested, since ecological phenomena are often spatially or temporally correlated and their frequency distributions are rarely normal (Rossi et al. 1992). Recently, a branch of applied statistics, known as geostatistics, has been demonstrated to be useful for determining spatial correlations among ecological data and for estimating values at unsampled locations (e.g., Robertson 1987, Robertson et al. 1988, Rossi et al. 1992).

Objectives of this study were (1) to use geostatistics to describe and model the spatial continuity of soil variables around individual plants, (2) to use this information to produce graphical representations or maps of specific resource islands, and, finally, (3) to quantify the spatial correlation between plants and soil variables. We examined *Artemisia tridentata* (sagebrush), a prominent shrub of cool desert environments (West 1983) previously known to affect the distribution of resources in the soil. Several workers have measured higher concentrations of resources such as total-C, total-N, inorganic-N, and higher rates of N cycling in soil beneath *A. tridentata* than in nearby open soil using a binary sampling regime (e.g., Burke 1989, Burke et al. 1989, Bolton et al. 1990, 1993). However, these studies have not accounted for possible spatial autocorrelation of the samples, evaluated resource islands of individual plants, nor quantified the scale of soil heterogeneity beneath *A. tridentata*.

Geostatistics has previously been used to describe environmental and soil parameters associated with *A. tridentata*. For example, Pierson and Wight (1991) used one-dimensional geostatistics to analyze spatial and temporal variability of soil temperature under *A. tridentata*. Halvorson et al. (1992) demonstrated that geostatistics was an appropriate means of measuring resource islands at the scale of an individual *A. tridentata* plant. Jackson and Caldwell (1993a) attempted to quantify the scale of nutrient heterogeneity around individual *A. tridentata* and *Pseudoroegneria spicata* in a native sagebrush steppe using semivariograms. They demonstrated increasing autocorrelation of soil nutrients at spatial scales <1 m but did not determine whether small-scale effects were attributable to individual plants or an artifact of the nested sampling design used. More recently, they constructed kriged maps that showed relatively high concentrations of soil variables like soil organic matter, extractable phosphate, and potassium near *Pseudoroegneria* tussocks but not *Artemisia* shrubs (Jackson and Caldwell 1993b). However, these kriged maps did not directly quantify spatial covariation between locations of individual plants and resource islands. Further, Jackson and Caldwell did not observe autocorrelation for microbial processes at any scale that was measured.

To meet our objectives, we applied geostatistics in three steps. First, we characterized and modeled the similarity between samples as a function of their separation distance and direction. Second, we used this relationship to interpolate values at unsampled locations directly under and near individual plants. Finally, we quantified spatial covariation between soil properties and plants.

STUDY SITE

The study was conducted at the Arid Land Ecology (ALE) Reserve, located on the Hanford Site in south central Washington (see Bolton et al. 1990 for details). There, remnants of the native *Artemisia tridentata–Elytrigia spicata* association occur on silt loams of the Warden or Ritzville series. This perennial shrub-steppe is the largest grassland-type in

North America and covers more than 640,000 km^2 of the Intermountain Pacific Northwest too dry to support forests (Daubenmire 1970, Rogers and Rickard 1988). In an undisturbed state the *A. tridentata–E. spicata* association would be composed typically of three layers of vegetation: an overstory shrub (*Artemisia tridentata tridentata*), a large caespitose perennial grass (*Elytrigia spicata* [formerly *Agropyron spicatum*]), and a small caespitose perennial grass (*Poa secunda*) growing on soil with a thin cryptogamic crust (Daubenmire 1970). However, following disturbance such as tillage, grazing, or fire, the alien annual grass *Bromus tectorum* becomes established.

METHODS

Soil Collection and Analysis

Cores of surface soil (10.5 cm dia. × 5 cm deep) were collected at 41 specific locations within 2 × 2-m plots centered on mature *A. tridentata* individuals (Fig. 1). Samples were located so as to minimize the number of data points needed for analysis of spatial characteristics and to avoid preferential clustering. We sampled five identically oriented plots (205 points) in March 1991, when levels of soil moisture and microbial biomass activity were high. All plots were located within approximately 20 m of each other within a flat area with randomly spaced plants. Multiple plots were sampled for two reasons: first, to assess spatial characteristics of resource islands by basing our calculations on several examples rather than a single instance; and, second, to provide replicates in the event that no spatial dependence of soil properties was observed. Data from all plots were combined to consider spatial dependence of soil properties around several *A. tridentata* plants simultaneously. This approach was chosen because it provided a more generalized evaluation of resource islands under individual *A. tridentata* and greatly increased the number of data pairs at any separation distance.

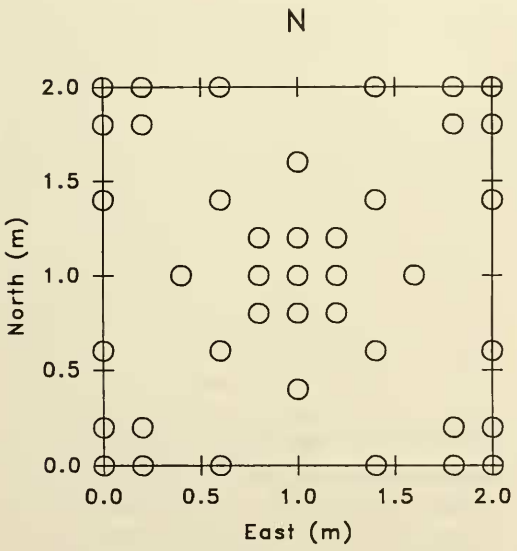

Fig. 1. Schematic of a typical sampling plot. Each plot (five total) was centered on an *Artemisia tridentata* plant. Dashed circles show the location of 41 soil cores (10.5 cm dia. × 5 cm deep). All five plots were oriented as shown.

Estimates of plant location were required for cross variography (see below). Therefore, vegetation maps were produced from vertical photographs. Each plot was divided into 5 × 5-cm squares. Each square was classified into one of three groupings—bare, grass species, or *A. tridentata*—based on predominant coverage. For this work no attempt was made to distinguish among grass species.

Each soil sample was sieved (5 mm), mixed, and analyzed for a variety of soil variables. For this work we present data only for water-soluble forms of C, total inorganic-N (i.e., nitrate + ammonium), and soil microbial biomass-C. Soluble soil C (H_2O-C) was extracted with room temperature deionized water and analyzed using an infrared gas analyzer (Ionics Inc., Watertown, Massachusetts). Total inorganic nitrogen (TI-N) was extracted within 48 h of collection from 10-g subsamples of soil using 25 ml 2M KCl and analyzed colorimetrically (Alpkem Corp., Clackamas, Oregon). Soil microbial biomass-C (SIR-C) was estimated from the respiratory response of soil to glucose, a source of C readily utilized by heterotrophic soil microorganisms (Anderson and Domsch 1978). Ten-gram samples of soil were placed in 40-ml glass vials, moistened with deionized H_2O, covered with Parafilm, and incubated in the dark at 23.5 ± 0.5°C for 1 wk. Each sample was then amended with a glucose solution at the rate of 600 mg glucose (240 mg C) kg^{-1} soil, bringing the final H_2O content of the soil to 20–25% (w/w; equivalent to 30–50 kPa). Glass vials were sealed with silicone septa and incubated for 3 h. Soil respiration was measured by gas chromatography and related to

estimates of soil microbial biomass-C with equations developed by Anderson and Domsch (1978).

Univariate Statistics

Univariate statistics were calculated for each soil parameter. For classical inferential statistics, data were also assigned to one of five distance classes depending upon sample location within a plot. These classes can be envisioned as concentric rings located at increasing distances from the center of the plot. The first distance class comprised samples collected directly under *A. tridentata* (distance = 0 cm, n = 1 per plot), followed by the second (approximate distance = 25 cm, n = 8 per plot), third (approximate distance = 60 cm, n = 8 per plot), fourth (approximate distance = 110 cm, n = 12 per plot), and fifth (approximate distance = 130 cm, n = 12 per plot). Average values of soil properties in each distance class were plotted as a function of radial distance from the plant axis. Following variography (see below), $\log_{10}$ transformed samples deemed spatially independent were compared with ANOVA using plot as a blocking factor.

Geostatistics

VARIOGRAPHY.—We evaluated spatial characteristics of each soil parameter with the nonergodic autocorrelation function (Srivastava and Parker 1989) and summarized results graphically as correlograms. Like variograms, correlograms represent the average degree of similarity between samples as a function of their separation distance (lag) and direction. Unlike the variogram, the correlogram filters out the effects of changes in both lag means and lag variances. Each point in a correlogram was calculated from this equation:

$$\rho^*(h) = \frac{1}{N(h)} \cdot \frac{\sum_{i=1}^{N(h)} \{[z(x_i) - m_{-h}][z(x_i+h) - m_{+h}]\}}{S_{-h}\, S_{+h}} \quad (1)$$

where $z(x_i)$ and $z(x_i + h)$ are two data points separated by the distance (lag) h. Datum $z(x_i)$ is the tail and $z(x_i + h)$ is the head of the vector, N(h) is the total number of data pairs separated by lag h, m_{-h} and m_{+h} are means of the points that correspond to tail and head of the lag, respectively, and S_{-h} and S_{+h} are standard deviations of tail and head values of the lag, respectively. We chose the correlogram because it removes the effects of lag means and standardizes by the lag variances (Rossi et al. 1992). For this work we express correlograms in the form of a standardized variogram by subtracting each $\rho^*(h)$ from 1 (Isaaks and Srivastava 1989, Rossi et al. 1992).

Correlograms were first calculated solely as a function of lag distance (i.e., the omnidirectional case) without considering any differences in spatial continuity with direction (i.e., anisotropy). However, since resource islands need not be symmetric (e.g., Zinke 1962), we also calculated directional correlograms. For each soil property a separate correlogram was calculated for samples oriented 0°, 45°, 90°, and 135° (±15° tolerance) from each other. Since correlograms are symmetric about the origin (i.e., 0° = 180°, 45° = 225°, etc.), 0°, 45°, 90°, and 135° directions correspond to samples aligned along east-west, northeast-southwest, north-south, and northwest-southeast axes.

Because the data of each plot were concatenated during this analysis, local anisotropies (i.e., anisotropies specific to each plot) were in effect combined. Thus, any directional effects we observed were a composite of the five plots and presumably indicative of overall directional trends. To identify directions of maximum and minimum continuity, we estimated the lag distance corresponding to a common value for each directional correlogram (Isaaks and Srivastava 1989). The directional correlogram with the greatest lag associated with a correlogram value of 1 was identified as the direction of greatest continuity. The correlogram with the smallest lag corresponding to 1 was deemed the direction of minimum continuity.

The empirically determined scatter of data points in each correlogram was fit with models known to produce a positive definite kriging system (i.e., matrices that provide both a unique solution and a positive estimation variance; Isaaks and Srivastava 1989). Such models typically contain several salient features known as nugget, range, and sill. The **nugget** is the amount of variance not explained or modeled as spatial correlation. It is the *apparent* ordinate intercept and is due to (1) unsampled correlation below the smallest lag and (2) experimental error (Rossi et al. 1992). A small nugget relative to the sill indicates that a large pro-

portion of the sample variability is modeled as spatial dependence. Conversely, a large nugget indicates less sample variability can be modeled as spatial dependence. The **sill** is characterized by a leveling off of the correlogram model. If present, it indicates that spatial correlation is, on average, constant. However, if spatial correlation continues to change at lags greater than those considered in the correlogram, then a sill will not be apparent. The lag value when the correlogram model reaches the sill is known as the **range**. It represents the maximum separation distance within which samples are spatially correlated. At lags ≥ the range, the sill of the variogram may approach the sample variance (Barnes 1991).

KRIGING TO ESTIMATE DATA AT UNSAMPLED LOCATIONS.—Kriging has been likened to "multiple linear regression with a few twists" (Rossi 1989). In classical multiple linear regression, an estimate of the dependent variable, Y, is calculated from a weighted linear combination of independent variables where each is measured at about the same location in time or space. Usually, only a single value of Y is estimated. Similarly, in kriging, $z^*(x_o)$, the estimated value of the variable for an unsampled location (x_o), is calculated as a weighted linear combination of the surrounding sampled neighbors:

$$z^*(x_o) = \sum_{i=1}^{N} g_i \cdot z(x_i) \qquad (2)$$

where the $z(x_i)$'s are the sampled values at their respective locations, and the g_i's are the weights associated with each sample value. In ordinary kriging, weights used to estimate $z^*(x_o)$ are chosen so that the resulting estimate is unbiased and has a minimum estimation variance and sum to unity. Kriging incorporates a model of spatial continuity (here the correlogram model) and accounts for the degree of clustering of nearby samples and their distance to the point being estimated (Isaaks and Srivastava 1989). We used ordinary point kriging to estimate values of soil properties at unsampled locations. For each plot we estimated values for the nodes of a 5 × 5-cm^2 grid. Each predicted value was based on a minimum of 6 and a maximum of 12 neighbors located within a 0.8-m circular search radius.

CROSS-VARIOGRAPHY.—In addition to spatial characteristics of single soil properties, we also determined how soil properties covaried with plants. We modeled spatial covariation with $\rho^*_{AB}(h)$, the estimated nonergodic cross-correlogram. Like the correlogram, it accounts for both variables' fluctuating lag means and variances (Isaaks and Srivastava 1989, Rossi et al. 1992). Because comparisons between continuous variables (i.e., TI-N, SIR-C, and H_2O-C data) and discrete variables (i.e., plant data) might be complicated by a "contact effect" (Luster 1985), we converted TI-N, SIR-C, and H_2O-C data to binary variables using an indicator transformation (Journel 1983). For this work, continuous data values of TI-N, SIR-C, and H_2O-C were coded 1 if they were greater than the local (within-plot) median, or 0 following Halvorson et al. (in review). Cross-correlograms were then calculated for grass species or *A. tridentata* and indicator transformed TI-N, SIR-C, and H_2O-C data using the equation,

$$\rho^*_{AB}(h) = \frac{1}{N(h)} \cdot \frac{\sum_{i=1}^{N(h)} \sum_{k=1}^{N(h)} [I_A(x_i,z_A) - m_{A_{-h}}][I_B(x_k,z_B) - m_{B_{+h}}]}{S_{A_{-h}} S_{B_{+h}}} \qquad (3)$$

where $N(h)$ is the total number of data pairs separated by vector h, $I_A(x_i,z_A)$ is the coded plant data (equal to 1 if the specified plant type was present or 0 if absent) at some location (x_i), $m_{A_{-h}}$ and $S_{A_{-h}}$ are the mean and standard deviation, respectively, for the plant variable at those data locations that are –h away from a soil property data location. Similarly, $I_B(x_k,z_B)$ is the coded soil variable data (equal to 1 if the data value is greater than the local plot median or else 0) at location (x_k), $m_{B_{+h}}$ and $S_{B_{+h}}$ are the mean and standard deviation of the soil variable indicator calculated for those locations that are +h away from a plant variable data location. Note, when h is 0, equation 3 is equivalent to the Pearson correlation coefficient (Isaaks and Srivastava 1989).

Unlike the correlogram, values calculated for the cross-correlogram may not be symmetric about the origin because both the order and direction are switched when variables are reversed (Isaaks and Srivastava 1989). Consequently, we calculated individual cross-correlograms for the 0°, 45°, 90°, 135°, 180°, 225°,

270°, and 315° directions (±30° tolerance). These correspond to soil samples aligned to the east, northeast, north, northwest, west, southwest, south, or southeast of a plant.

RESULTS

Summary statistics indicated that samples of TI-N and H_2O-C were positively skewed, while samples of SIR-C were more normally distributed (Figs. 2A–C). Total inorganic-N ranged from 0.6 mg / kg soil to a maximum of 23.6 mg / kg soil (Fig. 2A). The mean value for TI-N of 3.8 mg / kg soil compared reasonably to the values reported by Bolton et al. (1990) of 4.1 and 4.9 mg / kg soil for open soil crust and *A. tridentata* soil, respectively. Values observed for H_2O-C ranged widely from 9.8 mg / kg soil to 633.9 mg / kg soil (Fig. 2B). Estimates of SIR-C ranged from less than 200 to over 1800 mg / kg soil (Fig. 2C). The average value for SIR-C, 750 mg/ kg, was within the range reported by Burke et al. (1989) and equivalent to about 980 kg C / ha soil assuming a bulk density of 1.3 (Bolton et al. 1990). Comparatively, Smith and Paul (1990) reported average microbial biomass pool size for grassland systems of 1090 kg C / ha.

Univariate statistics also indicated how soil properties varied with distance from the *A. tridentata* axis (i.e., center of the plot; Figs. 3A–C). Concentrations of H_2O-C and SIR-C were greatest within 25 cm of the plant axis and lowest at distances beyond 60 cm (Figs. 3B, C). A similar pattern was observed for TI-N except that mean concentration was low in soil collected from directly beneath the *A. tridentata* plant (Fig. 3A) and from distances beyond 60 cm. This somewhat unexpected finding of a resource "hole" in the center of the resource island may be indicative of differences in the cycling of N under sagebrush and grass plants.

Variography indicated that samples of TI-N, H_2O-C, and SIR-C were spatially correlated (Fig. 4). Correlograms for SIR-C and TI-N exhibited similar ranges of about 0.7 or 0.8 m. The correlogram for H_2O-C was similar to the others at small lag distances and equaled the sample variance at a range near 0.7 m. However, at greater lags, correlogram values for H_2O-C increased above the sample variance and did not appear to reach a sill until lags were greater than 1 m. A correlogram sill greater than 1 for H_2O-C can occur if the

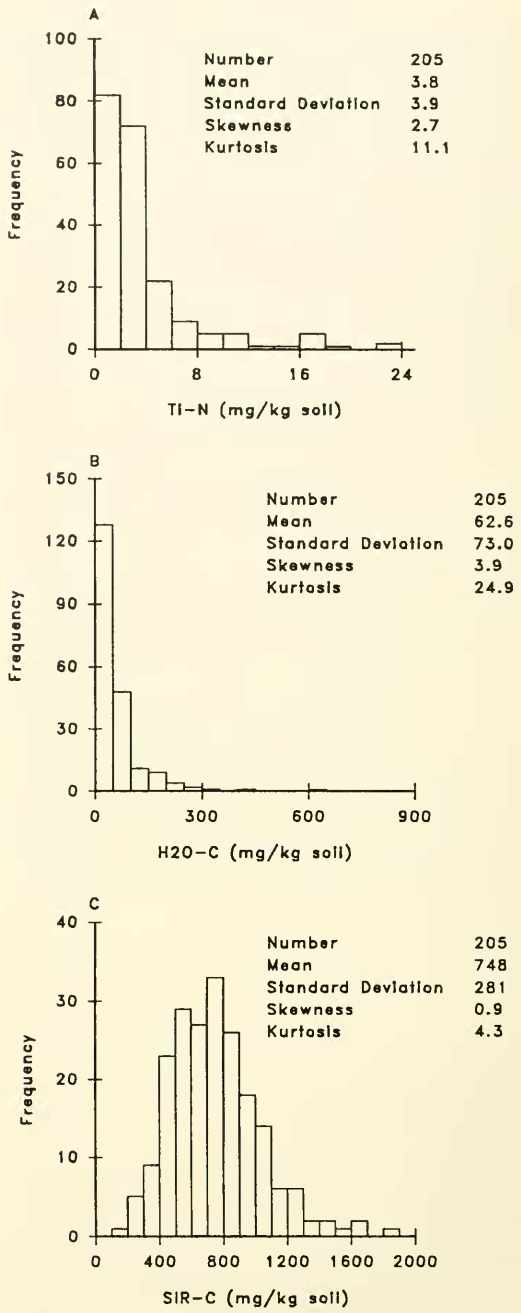

Fig. 2. Frequency histograms and some basic summary statistics for (A) total inorganic-N (TI-N), (B) water soluble-C (H_2O-C), and (C) soil microbial biomass-C (SIR-C).

majority of sample values are collected from an area with dimensions equal to or less than the variogram range (Barnes 1991) or if discrete regions of high and low concentration occur at lags greater than the maximum lag in

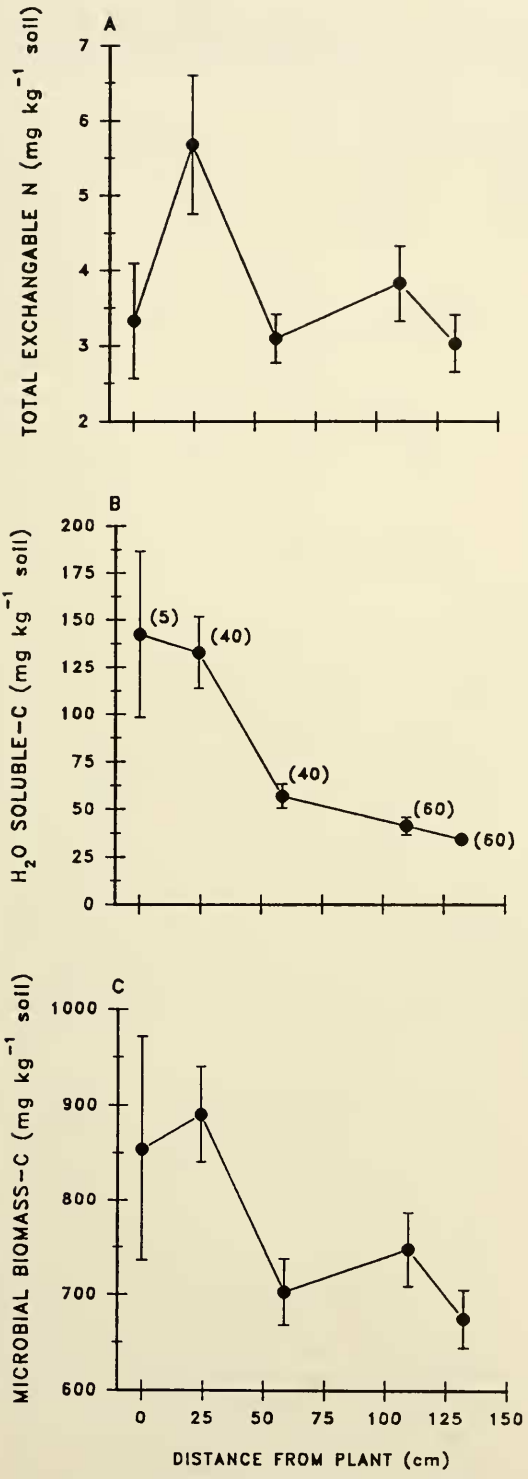

Fig. 3. Mean ± standard error for (A) TI-N, (B) H_2O-C, and (C) SIR-C. Numbers in parentheses are the number of data points (from five plots combined) that contribute to each estimate.

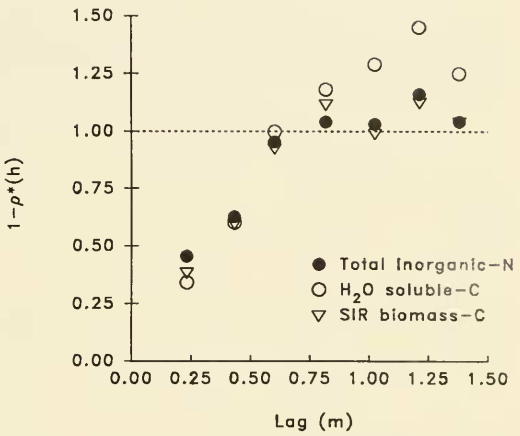

Fig. 4. Omnidirectional correlograms for TI-N, H_2O-C, and SIR-C. Each point shown was calculated from a minimum of 253 pairs (range 253–644).

the correlogram (i.e., an incompletely modeled "hole" effect). The apparent nuggets for all three soil parameters suggested that more than 75% (a correlogram value of 0.25 or less) of total sample variability could be modeled as spatial dependence.

Ranges observed in correlograms of soil properties were used to establish the separation distance beyond which correlation between samples could not be distinguished from sample variance. In other words, samples separated by distances greater than the range were candidates for analysis using more traditional statistical techniques that assume independence such as ANOVA. For our data, samples in the first two distance classes were thus combined and compared to samples from the last two classes because they were separated by more than about 0.8 m. Samples in the third distance class, lying at an intermediate distance between the center and outer boundary of the plot, were excluded from analysis. Analysis of variance of $\log_{10}$ transformed data using the five plots as blocking factors showed mean concentrations of TI-N, H_2O-C, and SIR-C to be significantly greater ($P < .001$) within 29 cm of the plant axis than values collected ≥ 1.07 m away from the plant axis (Table 1).

Omnidirectional correlograms characterized spatial correlation or continuity purely as a function of lag distance. However, by considering the orientation of samples in addition to their lag distance, directional anisotropies were suggested. Directional correlograms showed

TABLE 1. Summary statistics and randomized complete block ANOVAs for $\log_{10}$ transformed TI-N, H_2O-C, and SIR-C. Data are summarized into two sample location classes: **Near** (all measurements collected from within 29 cm of the plant axis; $n = 45$) and **Away** (samples collected at distances greater than 107 cm from the plant axis; $n = 120$). Average separation distance between the two location classes was 99.4 cm.

	Mean		Standard deviation		Standard error	
	Near	Away	Near	Away	Near	Away
TI-N	0.58	0.39	0.34	0.32	0.05	0.03
H_2O-C	2.01	1.49	0.31	0.26	0.05	0.02
SIR-C	2.93	2.82	0.14	0.17	0.02	0.02

	Source of variation	df	MS	*F*	*P*
	Plot	4	0.59	6.14	<.001
TI-N	Sample Location	1	1.14	11.81	.001
	Error	159	0.10		
	Plot	4	0.21	2.85	.026
H_2O-C	Sample Location	1	8.79	122.49	<.001
	Error	159	0.07		
	Plot	4	0.06	2.32	.060
SIR-C	Sample Location	1	0.36	13.63	<.001
	Error	159	0.03		

differences in both nuggets and ranges (Fig. 5). Generally, the largest apparent nuggets were observed in correlograms oriented in the 0° (east-west) and 45° (northeast-southwest) directions. With the exception of H_2O-C, these correlograms had estimated nuggets of 0.4 or more. Conversely, correlograms calculated for the 90° (north-south) and 135° (northwest-southeast) directions generally exhibited nuggets of ≤ 0.2.

Directions of maximum and minimum continuity were identified. For TI-N, maximum continuity was observed in the 45° direction while lower but similar ranges of continuity were observed in the other three directional correlograms (Fig. 5, left column). Little anisotropy was observed in directional correlograms for H_2O-C, suggesting that spatial correlation could be adequately modeled with a single isotropic correlogram (Fig. 5, center column). Like TI-N, the direction of maximum continuity observed for SIR-C was 45°, with a direction of minimum continuity in the 135° direction (Fig. 5, right column). The anisotropies for TI-N and SIR-C were accounted for in kriging by using a model that evaluated both distance and direction (Table 2).

Maps of the estimates generated with these models and ordinary kriging were constructed for each soil property in each plot. Taken together they suggest that generalizations about spatial distribution of resources in the soil beneath *A. tridentata* can be complicated by the variation observed between individual plants and specific soil properties. For example, distinct "islands" of TI-N were not always clearly associated with *A. tridentata.* Instead, in three of five plots highest concentrations of TI-N appeared to be associated with location of grasses (Fig. 6, plots A,B,E). In plots C and D, concentrations of TI-N were highest in the vicinity of the *A. tridentata* canopy. However, vegetation maps of these plots indicate that grass species were present near the *A. tridentata* plant. In plot E smallest concentrations of TI-N were predicted to lie under the *A. tridentata* plant.

Conversely, highest accumulations of H_2O-C were clearly associated with *A. tridentata* in kriged maps. In each plot high concentrations of H_2O-C were localized near the plot center under the plant canopy. Location of grass species did not always appear to coincide strongly with high concentrations of H_2O-C (see NW 1/4 of plot A, NE and SE 1/4 of plot B, and NE 1/4 of plot E). However, high concentrations of both TI-N, and H_2O-C did coincide with location of grasses in the NW 1/4 of plot B and SW 1/4 of plot E.

Maps of SIR-C indicate that islands of soil biomass-C were present under plants but not apparently specific to any particular type of vegetation. Relatively high concentrations of SIR-C were estimated under *A. tridentata* plants in all plots. However, SIR-C was also

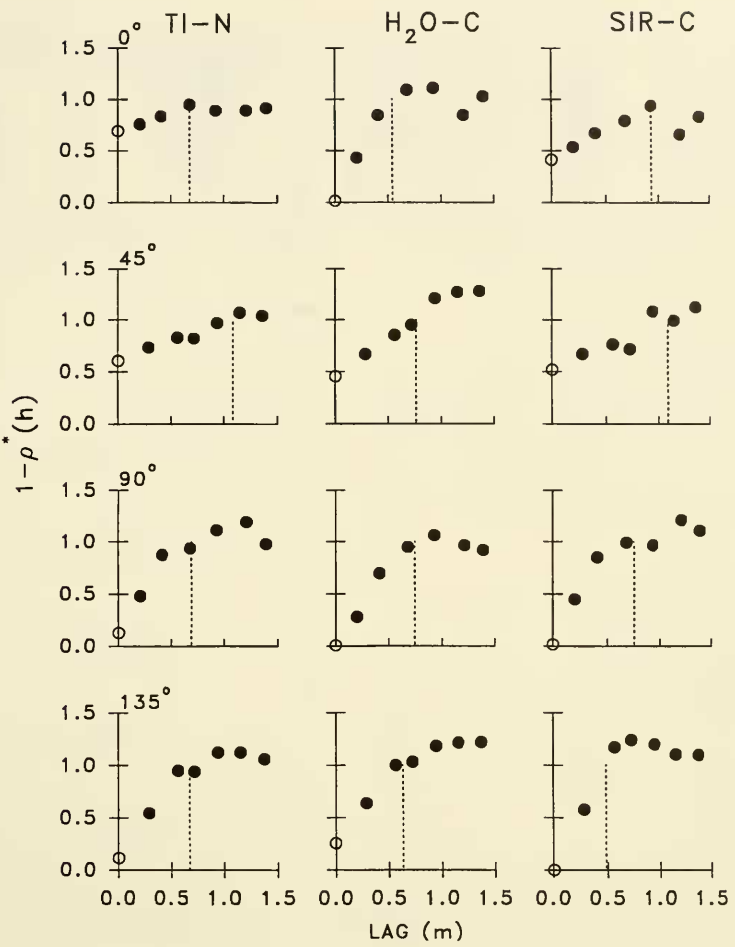

Fig. 5. Directional correlograms for TI-N, H_2O-C, and SIR-C in the 0°, 45°, 90°, and 135° directions calculated with a tolerance of ±15°. Each point shown was calculated from a minimum of 47 pairs (range 47–212). Vertical lines correspond to a correlogram value of 1 and were used to identify directions of maximum and minimum spatial continuity. Open symbols are estimates of the apparent nugget (the apparent ordinate) fit by eye.

accumulated elsewhere in relation to the location of grass species. High concentrations of SIR-C were observed in several instances not associated with high concentrations of either TI-N or H_2O-C (e.g., NE and SW 1/4 of plot B, NW 1/4 of plot D).

Cross-variography indicated how TI-N, H_2O-C, and SIR-C covaried spatially with respect to *A. tridentata* and grass species. Indicator transformed TI-N data were similarly and positively correlated with *A. tridentata* and grass species at a lag of 0 (equivalent to the Pearson correlation coefficient; Figs. 7A,B). However, correlation varied with increasing lag distance (i.e., showed spatial dependence) in a different manner for each. For *A. tridentata* highest positive correlations with TI-N were observed in the 45° (northeast) and 90° (north) directions (Fig. 7A). The range over which *A. tridentata* remained positively correlated with TI-N was longest in the 45° and 90° directions, extending to about 1 m and 0.75 m, respectively. Positive correlations with TI-N were observed for other directions too but only to a lag of about 0.5 m. In contrast, grass species were positively correlated to above-median TI-N concentrations in the 315° (southeast), 270° (south), and 225° (southwest) directions (Fig. 7B). The range over which grass species were positively correlated to TI-N in these directions was less than that for *A. tridentata*. In other directions grass species were uncorrelated or negatively correlated to TI-N at lags above 0.

TABLE 2. Model[1,2] parameters used for ordinary kriging ALE soil properties.

Soil parameter
TI-N
$1\text{-}\rho^*_{45}$ = .154 + 0.428 Sph(0.27) + 0.524 Sph(1.80)
$1\text{-}\rho^*_{135}$ = .154 + 0.428 Sph(0.71) + 0.524 Sph(1.20)
SIR-C
$1\text{-}\rho^*_{45}$ = .072 + 0.381 Sph(0.23) + 0.717 Sph(1.87)
$1\text{-}\rho^*_{135}$ = .072 + 0.381 Sph(0.74) + 0.717 Sph(0.75)
H_2O-C
$1\text{-}\rho^*$ = 1.40 Sph(1.3)

[1]Models shown for TI-N and SIR-C are a combination of a nugget constant and two spherical models. The spherical model, denoted "Sph," is an authorized model commonly used to model variograms. The number that precedes "Sph" can be thought of as the local sill for that model while the number in parentheses is the range at which the local sill is reached (see Isaaks and Srivastava 1989). For a correlogram, the standardized form is $1\text{-}\rho^*(h) = 1.5\,(\text{lag/range}) - 0.5\,(\text{lag/range})^3$ if lag ≤ = range, else 1 if otherwise.

[2]NOTE: Geostatisticians often distinguish between the nugget used for diagnostic purposes, which is the *apparent* ordinate intercept, and the nugget value, which is used in modeling.

Indicator transformed H_2O-C data were positively correlated with *A. tridentata* but not with grass species at a lag of 0 (Figs. 7C,D). As with TI-N, highest correlations with *A. tridentata* were observed in the 45° and 90° directions (Fig. 7C). Similar patterns of spatial dependence were observed for all directions. The distance to which H_2O-C remained positively correlated with *A. tridentata* ranged from a minimum of about 0.5 m to a maximum of near 0.75 m in the 45° and 90° directions. Unlike *A. tridentata*, H_2O-C was not positively correlated with grass species (Fig. 7D). Instead, H_2O-C was moderately negatively correlated in the 0°, 45°, 90°, and 135° directions, meaning grass species were more associated with below-median concentrations of H_2O-C. At lags greater than about 0.2 m, little change in cross-correlograms was observed, indicating only a weak spatial dependence.

In contrast to H_2O-C, cross-correlograms indicated that SIR-C was slightly more correlated with grass species than with *A. tridentata* at a lag of 0 (Figs. 7E,F). Like other soil properties, strongest positive correlation between *A. tridentata* and SIR-C was observed in the 45° direction, which also remained positively correlated to lags in excess of 1 m (Fig. 7E). Lowest correlations with *A. tridentata* were to the 270° and 225° directions. Indicator transformed SIR-C data were most correlated to grass species in the 225°, 270°, and 315° directions (Fig. 7F). Spatial dependence of correlations was observed out to a lag of about 0.5 m. Beyond this, correlations of grass species with SIR-C remained approximately constant.

DISCUSSION

Geostatistics can be applied to resource island data to provide several useful diagnostic features prior to actual mapping of the landscape itself. For example, variography can define the presence and extent of spatial correlation and alert the researcher to apply with caution classical statistical comparisons that assume samples are independent and from identically distributed populations. For these methods to be more properly applied to spatial data, comparisons should probably be limited to those samples separated by distances ≥ range of the correlogram (Table 1; Webster 1985, Robertson 1987). This is true for studies that compare samples collected along a continuum such as distance, depth, or concentration (i.e., resource gradient) or as a function of time.

Another promising use of variography is to relate spatial continuity of two or more variables at the same site or the same variable at two or more sites by comparing variograms, covariograms, or correlograms with one another. This approach may be useful for comparing the scale of ecological processes or ecosystem boundaries, but should be approached with caution for several reasons. First, each point in a traditional variogram represents the *average* value of the squared difference between many pairs of data points. While an average value may be appropriate for modeling spatial continuity (as a summary statistic), it does not indicate the range of individual squared differences or provide an estimate of the "goodness of fit" about each point in a variogram. The range of the deviation about the average value may be large or small (see Webster and Oliver 1992), complicating comparisons of variograms. Thus, for comparative purposes other more "robust" representations of spatial dependence such as Journel's mAD estimator, Cressie-Hawkins' robust estimator, or the rodogram (see Rossi et al. 1992) may be more appropriate choices. Second, even if variograms for two properties are similar, resultant estimates may yield very different maps (e.g., TI-N and SIR-C in this study). This is because estimation of unknown data values by kriging depends not only

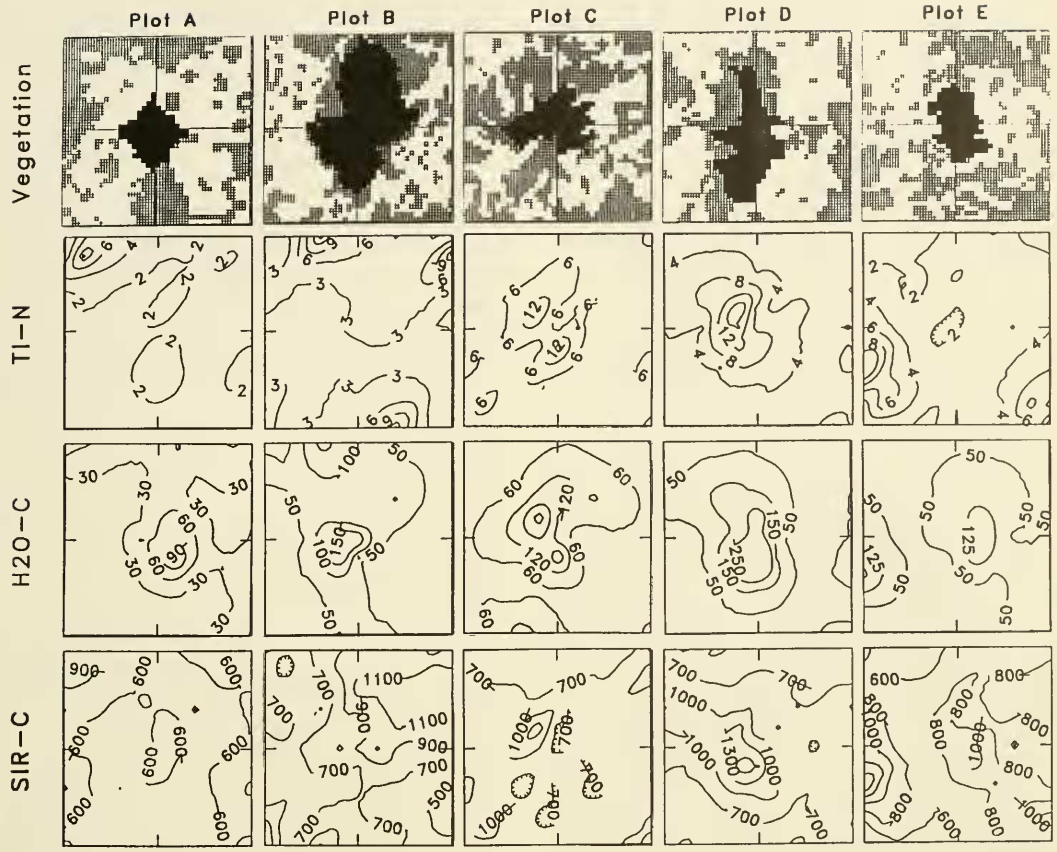

Fig. 6. 2 × 2-m maps of vegetation and kriged estimates of Tl-N, H_2O-C, and SIR-C for five ALE plots. Each kriged plot is composed of 1681 points estimated by ordinary point kriging. Vegetation maps indicate vertical projections of *A. tridentata* (black) and grass species (crosshatch) as determined from photographs. Soil properties are depicted in mg / kg soil (dw).

upon a model of spatial continuity, but ultimately upon degree and configuration of the known sample values in the field.

During our analysis of resource island data using geostatistical methods, we made several assumptions or decisions about the data that could have affected our interpretations. First, we assumed that resource islands under *A. tridentata* could be monitored using a particular configuration of samples located within a 2 × 2-m plot. A different number of samples collected from a larger plot with a different shape or in a different pattern might have generated different correlogram models or kriged estimates (Webster and Oliver 1992). Second, we collected data at a single time during the year, thereby making the kriged maps "snapshots" in time and space. Data values and spatial continuity undoubtedly vary for some types of environmental variables (e.g., soil moisture or Tl-N) on a seasonal or shorter time scale. Other environmental variables such as soil texture, total-N, or C might change more slowly. Third, we chose to analyze data for the five plots collectively rather than for each plot individually. This choice reflects an interpretation that correlograms for individual plots were reasonably similar to each other and allowed our calculations to be based on a greater number of paired comparisons. We reasoned that correlogram models of spatial continuity, derived from concatenated data, would *summarize* typical patterns of spatial continuity and directional anisotropies. Alternatively, although single-plot analyses would result in plot-specific models of spatial continuity with greater specificity, they might make generalizations difficult. Finally, we assumed that spatial continuity for H_2O-C was reasonably described by a single isotropic model, but we concluded

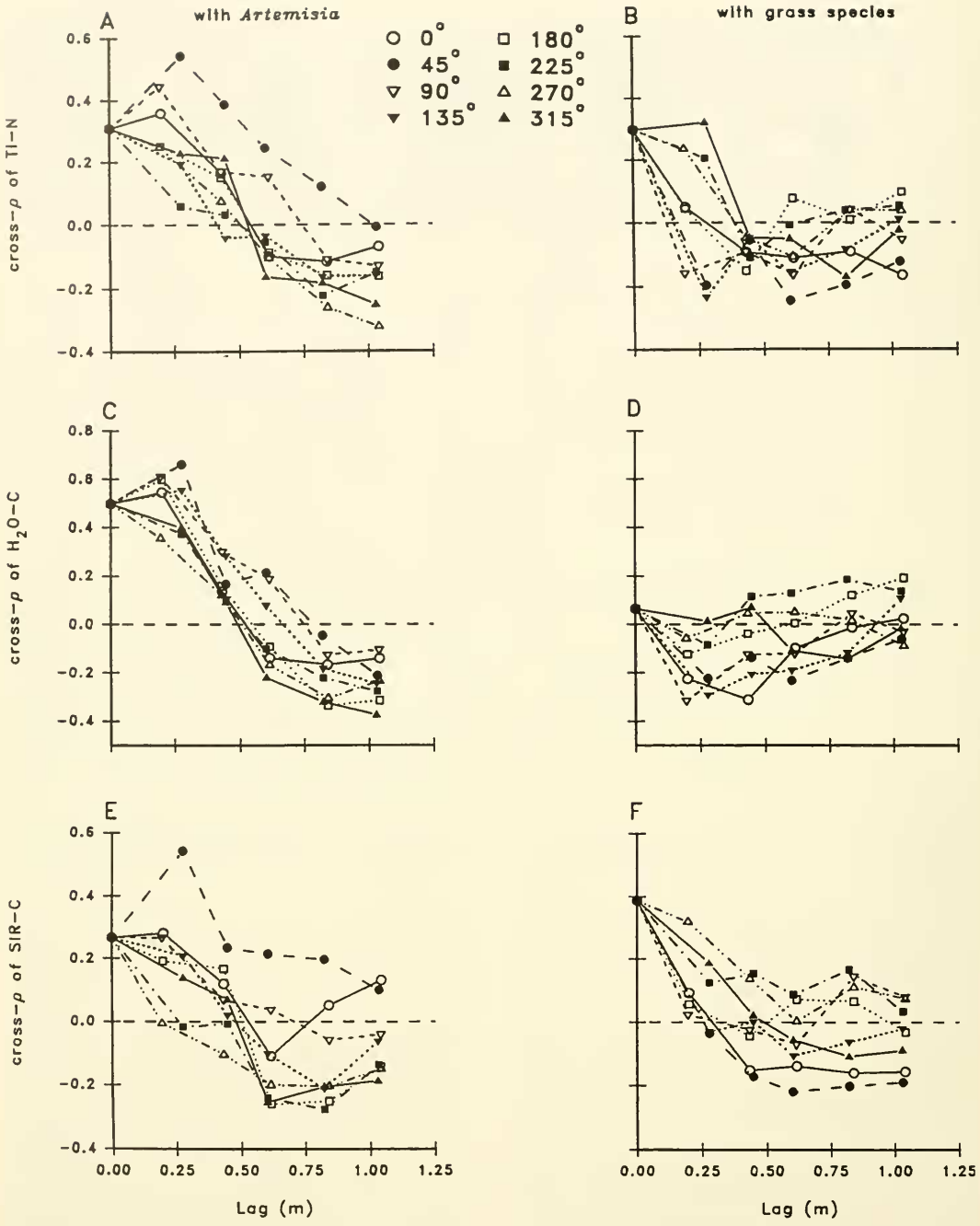

Fig. 7. Directional cross-correlograms showing spatial covariance of indicator transformed TI-N, H_2O-C, SIR-C data, and presence/absence (coded as 1 or 0) of *A. tridentata* and grass species. Correlograms were calculated for 0° (east), 45° (northeast), 90° (north), 135° (northwest), 180° (west), 225° (southwest), 270° (south), and 315° (southeast) directions ±30° tolerance. Each point shown summarizes a minimum of 54 pairs (range 54–158).

that directional anisotropies observed for TI-N and SIR-C were important enough to be accounted for in the estimation process.

Results of a geostatistical analysis cannot completely replace "sound ecological reasoning" or theory (Rossi et al. 1992). Thus, the researcher must decide whether directional anisotropies observed in descriptive variography portray significant spatial patterns or are merely a coincidental result of the number and arrangement of data. The decision to account for spatial anisotropy in the kriging procedure is, in part, related to the desired end product of the geostatistical analysis. For example, if the goal of an analysis is the most accurate representation possible of a particular resource island under a specific *A. tridentata*, then a highly detailed model of spatial continuity would be appropriate regardless of the source of spatial variability. In this case variography based on a concatenated data set might be less appropriate than analysis based only on the single plot. However, the goal of geostatistical interpretation of ecological data may not be to produce detailed site maps. Instead, the ecologist may be more interested in patterns that are broadly applicable. Anisotropies can often be related to information about the environment such as stratigraphic, meteorological, or hydrogeological patterns (Isaaks and Srivastava 1989) and may suggest linkages between environmental variables. Our decision to account for anisotropies in the kriging process was, in part, influenced by information about another environmental parameter, prevailing wind direction. For this reason we would expect the anisotropies observed for TI-N and SIR-C to be a consistent feature of the ALE landscape.

Directional correlograms revealed greatest spatial continuity for samples of TI-N and SIR-C in the 45° direction, northeast-southwest. Cross-correlograms, more specifically, indicated that above-median concentrations of soil properties were most correlated to *A. tridentata* in the 45° direction, or northeast. For the ALE site, cumulative records indicate that prevailing local wind direction is from the southwest quadrant (Table 3), corresponding to the downwind direction of greatest spatial continuity. Prevailing wind direction might influence spatial patterns of soil resources by affecting distribution of litter deposition which, for *A. tridentata* at the ALE site, may exceed 60 kg / ha annually (Mack 1971).

TABLE 3. Frequency of occurrence of wind at the ALE site. Source: H. Bolton, Pacific Northwest Laboratory.

Source quadrant	1990		1991	
	Hours	Percent	Hours	Percent
0–90° (NE)	1161	13.25	1208	13.97
90–180° (SE)	1557	17.78	1613	18.66
180–270° (SW)	4090	46.70	3974	45.96
270–360° (NW)	2227	22.27	1851	21.41

Evidence for the occurrence of resource islands in the ALE landscape was provided by comparing concentrations of soil resources collected near *A. tridentata* vegetation to those collected away from the plant. However, the specific sampling regime employed to evaluate "near" vs. "away" influenced the particular conclusion reached. For example, Bolton et al. (1990) were unable to conclude that concentrations of TI-N in soil under *A. tridentata* were significantly greater than concentrations measured in open soil crust based on six samples drawn at random from each soil type (see also Doescher et al. 1984). In contrast, we found that evaluating TI-N vs. distance away from the *A. tridentata* axis resulted in the naive conclusion that significantly higher concentrations of TI-N would always occur under *A. tridentata* plants (Fig. 3A, Table 1). Such a conclusion for TI-N and other soil properties would lead to a model of a landscape composed of identically sized, symmetrical resource islands centered on each *A. tridentata* individual and would infer some sort of causal relationship between concentration of TI-N and *A. tridentata* presence. However, kriged maps suggest that greatest concentrations of TI-N were not always associated with *A. tridentata*.

Autocorrelation of soil properties was described using variography. The association of soil variables with *A. tridentata* individuals was supported jointly by kriged maps and cross-correlograms, with the latter showing that soil properties (especially H_2O-C) were positively correlated to *A. tridentata*. Kriging is a means for producing visually satisfying maps of soil properties and provided additional insight into characteristics of resource distribution under *A. tridentata*. However, we relied on these maps primarily as heuristic tools because we recognized that kriged maps

are models that can be influenced by decisions about the data set (e.g., concatenated vs. single plot), the "art" of variogram modeling, the type of kriging chosen (ordinary kriging is a data "smoother"), the specific search strategy used, and the method of graphical representation. Finally, kriging by itself does not provide a measure of estimate confidence or reliability like nonparametric methods (Journel 1983) or stochastic conditional simulation (Rossi et al. 1993).

Kriged maps of H_2O-C appeared to be most similar to graphs of summary statistics vs. distance from plant axis (Fig. 3A). In each kriged map (Fig. 6), high concentrations coincided with *A. tridentata* in a classic resource island pattern. These accumulations might be tied closely to inputs from *A. tridentata* litter fall representing a source of C that could be accessed by heterotrophic soil microorganisms. Alternatively, high concentrations of H_2O-C under *A. tridentata* might not indicate large C inputs. Instead, they might indicate the accretion of soluble, but recalcitrant, forms of C not readily useable by soil microorganisms. In this case the term "resource island" would be ambiguous. To have ecological significance, a resource island must be evaluated for resource quantity, resource quality, and presence of alternative resource substitutes. Further, the significance of resource accumulation into islands might change with time in relation to diurnal cycles, growing season, or successional stage (Halvorson et al. 1991).

Kriged maps of SIR-C showed accumulations of soil microbial biomass in close proximity to each *A. tridentata* individual. However, high concentrations were also observed for locations corresponding to other plant species, demonstrating that resource islands of microbial populations or activity can be numerous and are nonspecific to *A. tridentata*. Additionally, a significant amount of SIR-C was estimated for locations not associated with any plant. This suggests that while local inputs by plants may stimulate microbial population growth or activity, sufficient resources exist in the environment to support moderate amounts of SIR-C during some times of the year. However, plant location may control the distribution of SIR-C indirectly through influence on microclimatological factors such as soil temperature and evapotranspiration. These factors would become more important during the hot, dry summer months and could limit distribution of SIR-C to locales closer to *A. tridentata*.

Assessing the distribution of soil microbial populations or microbially mediated nutrient-cycling processes such as mineralization or denitrification is complicated by multiple resource requirements and compensatory capabilities of living microorganisms (Smith et al. 1985). For example, microbial population size or activity within a C-substrate resource island might be limited by the availability of soil N. Conversely, the same microbial population might be limited by the availability of C-substrate despite an N-rich environment. Under such a scenario the greatest population size or activity might occur in a location with low or intermediate quantities of both C and N, and the resource island for soil microorganisms or mineralization potential would appear distinct spatially from other resources. Estimation of soil properties like SIR-C that depend on the distribution of one or more other resources may need to be evaluated with respect to temporal and spatial distributions of alternative resources.

Kriged maps of various soil properties can be interpreted within the context of the relationship between the particular soil parameter and *A. tridentata*. Our data indicate that shape and orientation of resource islands under *A. tridentata* vary with the specific soil property considered, need not be centered on the axis of an *A. tridentata* plant, and need not be symmetrical. The maps also provide evidence that suggests a vertical projection of the plant canopy is not well correlated to the distribution of soil variables and thus should not be used as a basis for sampling designs (Fig. 6). For some soil properties (e.g., H_2O-C) the difference between values characterizing the resource island and those characterizing the surrounding matrix may be large and the resource island may appear to have sharp boundaries. Conversely, the range of data values for other soil properties (e.g., SIR-C) may be smaller and the transition from resource island to the surrounding soil matrix more complicated. Resource island boundaries may also change with direction, making sampling designs based on only a few transects questionable. Finally, resource islands do not occur under all *A. tridentata* or for all soil properties.

Other plants like annual and perennial grasses can be the focal points for resource islands of some variables (Jackson and Caldwell 1993b).

Geostatistics allows estimation and mapping of resource islands in considerable detail. Such maps can be used to further our understanding of the ecology of *A. tridentata*, refine nutrient budgets for shrub-steppe ecosystems, reveal the existence of resource and process-dependent patterns, and help provide a rationale for sampling designs based on natural boundaries. Besides two-dimensional space, geostatistics can be used to consider differences in spatial continuity with soil depth (i.e., a third dimension) or time (via repeated measurements). However, even with geostatistics, our definition of a resource island can be improved. Whether a resource island is more properly delineated by some minimum difference in resource concentration or related to the ecological significance of small differences in concentration remains to be answered. Further, the resource island "effect" may be related to more than a single environmental parameter. Consequently, methods must be developed to simultaneously integrate information for several environmental variables and summarize them spatially.

ACKNOWLEDGMENTS

This research was supported in part by the Ecological Research Division, Office of Health and Environmental Research, U.S. Department of Energy (DOE). Pacific Northwest Laboratory is operated for the DOE by Battelle Memorial Institute under Contract DE-AC06-76RLO 1830. We thank Joe Aufdermaur, Debbie Bikfasy, Kirk Stallcop, and Jeff Sullivan for analytical assistance. M. W. Palmer and J. Price provided helpful editorial comments.

LITERATURE CITED

ANDERSON, J. P. E., AND K. H. DOMSCH. 1978. A physiological method for the quantitative measurement of microbial biomass in soils. Soil Biology and Biochemistry 10: 215–221.

BARNES, R. J. 1991. The variogram sill and the sample variance. Mathematical Geology 23: 673–678.

BARTH, R. C., AND J. O. KLEMMEDSON. 1978. Shrub induced spatial patterns of dry matter, nitrogen and organic carbon. Soil Science Society of America Journal 42: 804–809.

BELSKY, A. J., R. G. AMUNDSON, J. M. DUXBURY, S. J. RIHA, A. R. ALI, AND S. M. MWONGA. 1989. The effects of trees on their physical, chemical and biological environments in a semi-arid savanna in Kenya. Journal of Applied Ecology 26: 1005–1024.

BOLTON, H., JR., J. L. SMITH, AND S.O. LINK. 1993. Soil microbial biomass and activity of a disturbed and undisturbed shrub-steppe ecosystem. Soil Biology and Biochemistry 25: 545–552.

BOLTON, H., JR., J. L. SMITH, AND R. E. WILDUNG. 1990. Nitrogen mineralization potentials of shrub-steppe soils with different disturbance histories. Soil Science Society of America Journal 54: 887–891.

BURKE, I. C. 1989. Control of nitrogen mineralization in a sagebrush steppe landscape. Ecology 70: 1115–1126.

BURKE, I. C., W. A. REINERS, AND D. S. SCHIMEL. 1989. Organic matter turnover in a sagebrush steppe landscape. Biogeochemistry 7: 11–31.

CHARLEY, J. L., AND N. E. WEST. 1977. Micro-patterns of nitrogen mineralization activity in soils of some shrub dominated semi-desert ecosystems of Utah. Soil Biology and Biochemistry 9: 357–365.

COPPINGER, K. D., R. A. REINERS, I. C. BURKE, AND R. K. OLSON. 1991. Net erosion on a sagebrush steppe landscape as determined by Cesium-137 distribution. Soil Science Society of America Journal 55: 254–258.

DAUBENMIRE, R. 1970. Steppe vegetation of Washington. Technical Bulletin 62. Washington Agricultural Experiment Station, College of Agriculture, Washington State University, Pullman.

DAVIDSON, D. W., AND S. R. MORTON. 1984. Dispersal adaptations of some *Acacia* species in the Australian arid zone. Ecology 65: 1038–1051.

DOESCHER, P. S., L. E. EDDLEMAN, AND M. R. VAITKUS. 1987. Evaluation of soil nutrients, pH and organic matter in rangelands dominated by western juniper. Northwest Science 61: 97–102.

DOESCHER, P. S., R. E. MILLER, AND A. H. WINWARD. 1984. Soil chemical patterns under eastern Oregon plant communities dominated by big sagebrush. Soil Science Society of America Journal 48: 659–663.

EVERETT, R., S. SHARROW, AND D. THRAN. 1986. Soil nutrient distribution under and adjacent to singleleaf pinyon crowns. Soil Science Society of America Journal 50: 788–792.

FIREMAN, M., AND H. E. HAYWARD. 1952. Indicator significance of some shrubs in the Escalante Desert, Utah. Botanical Gazette 114: 143–155.

GARCIA-MOYA, E., AND C. M. MCKELL. 1970. Contributions of shrubs to the nitrogen economy of a desert wash plant community. Ecology 51: 81–88.

GARNER, W., AND Y. STEINBERGER. 1989. A proposed mechanism for the formation of 'fertile islands' in the desert ecosystem. Journal of Arid Environments 16: 257–262.

HALVORSON, J. J., H. BOLTON, JR., AND J. L. SMITH. 1992. Measurement of resource islands underneath *Artemisia tridentata*: a geostatistical approach. Pages 117–120 *in* Pacific Northwest Laboratory annual report. U.S. Department of Energy, Office of Scientific and Technical Information PNL-8000 UC-407:DE-AC06-76RLO 1830, Oak Ridge, Tennessee.

HALVORSON, J. J., J. L. SMITH, H. BOLTON, JR., AND R. E. ROSSI. In review. Defining resource islands using multiple variables and geostatistics.

HALVORSON J. J., J. L. SMITH, AND E. H. FRANZ. 1991. Lupine influence on soil carbon, nitrogen and

microbial activity in developing ecosystems at Mount St. Helens. Oecologia (Berlin) 87: 162–70.

HOOK, P. B., I. C. BURKE, AND W. K. LAUENROTH. 1991. Heterogeneity of soil and plant N and C associated with individual plants and openings in North American shortgrass steppe. Plant and Soil 138: 247–256.

ISAAKS, E. H., AND R. M. SRIVASTAVA. 1988. Spatial continuity measures for probabilistic and deterministic geostatistics. Mathematical Geology 20: 313–341.

_____. 1989. An introduction to applied geostatistics. Oxford University Press, New York.

JACKSON, R. B., AND M. M. CALDWELL. 1993a. The scale of nutrient heterogeneity around individual plants and its quantification with geostatistics. Ecology 74: 612–614.

_____. 1993b. Geostatistical patterns of soil heterogeneity around individual perennial plants. Journal of Ecology 1993 81: 683–692.

JENNY, H. 1980. The soil resource, origin and behavior. Springer-Verlag (Berlin).

JOURNEL, A. G. 1983. Nonparametric estimation of spatial distributions. Mathematical Geology 15: 445–468.

KOTLIAR, N. B., AND J. A. WIENS. 1990. Multiple scales of patchiness and patch structure: a hierarchical framework for the study of heterogeneity. Oikos 59: 253–260.

LUSTER, G. R. 1985. Raw materials for portland cement: applications of conditional simulation of coregionalization. Unpublished doctoral dissertation, Department of Earth Sciences, Stanford University, Stanford, California.

MACK, R. N. 1971. Mineral cycling in *Artemisia tridentata*. Unpublished doctoral dissertation, Washington State University, Pullman.

NISHITA, H., AND R.M. HAUG. 1973. Distribution of different forms of nitrogen in some desert soils. Soil Science 116: 51–58

PIERSON F. B., AND J. R. WIGHT. 1991. Variability of near-surface soil temperature on sagebrush rangeland. Journal of Range Management 44: 491–497.

REYNOLDS, J. F., R. A. VIRGINIA, AND J. M. CORNELIUS. 1990. Resource island formation associated with the desert shrubs, creosote bush (*Larrea tridentata*) and mesquite (*Prosopis glandulosa*) and its role in the stability of desert ecosystems: a simulation analysis. Supplement to Bulletin of the Ecological Society of America 70: 299–300.

ROBERTSON, G. P. 1987. Geostatistics in ecology: interpolating with known variance. Ecology 68: 744–748.

ROBERTSON, G. P., M. A. HUSTON, F. C. EVANS, AND J. M. TIEDJE. 1988. Spatial variability in a successional plant community: patterns of nitrogen availability. Ecology 69: 1517–1524.

ROGERS, L. E., AND W. H. RICKARD. 1988. Introduction: Shrub-steppe lands. Pages 1–12 *in* W. H. Rickard, L. E. Rogers, B. E. Vaughan, and S. F. Liebetrau, eds., Shrub-steppe, balance and change in a semi-arid terrestrial ecosystem. Elsevier, New York.

ROSSI, R. E. 1989. The geostatistical interpretation of ecological phenomena. Unpublished doctoral dissertation, Washington State University, Pullman.

ROSSI, R. E., P. W. BORTH, AND J. J. TOLLEFSON. 1993. Stochastic simulation for characterizing ecological spatial patterns and appraising risk. Ecological Applications 3: 719–735.

ROSSI, R. E., D. J. MULLA, A. G. JOURNEL, AND E. H. FRANZ. 1992. Geostatistical tools for modeling and interpreting ecological spatial dependence. Ecological Monographs 62: 277–314.

SCHLESINGER, W. H., J. F. REYNOLDS, G. L. CUNNINGHAM, L. F. HUENNEKE, W. M. JARRELL, R. A. VIRGINIA, AND W. G. WHITFORD. 1990. Biological feedbacks in global desertification. Science 247: 1043–1048.

SMITH J. L., AND E. A. PAUL. 1990. The significance of soil microbial biomass estimations in soil. Pages 357–396 *in* G. Stotzky and J. Bollag, eds., Soil biochemistry. Vol. 6. Marcel Dekker, New York.

SMITH, J. L., B. L. MCNEAL, AND H. H. CHENG. 1985. Estimation of soil microbial biomass: an analysis of the respiratory response of soils. Soil Biology and Biochemistry 17: 11–16.

SMITH, S. D., W. E. SMITH, AND D. T. PATTEN. 1987. Effects of artificially imposed shade on a Sonoran desert ecosystem: arthropod and soil chemistry responses. Journal of Arid Environments 13: 245–257.

SRIVASTAVA, R. M., AND H. M. PARKER. 1989. Robust measure of spatial continuity. Pages 295–308 *in* M. Armstrong, ed., Geostatistics. Vol. 1. Kluwer Academic, Dordrecht, The Netherlands.

VIRGINIA, R. A., AND W. M. JARRELL. 1983. Soil properties in a mesquite-dominated Sonoran desert ecosystem. Soil Science Society of America Journal 47: 138–144.

VIRGINIA, R. A., W. M. JARRELL, AND E. FRANCO-VIZCAINO. 1982. Direct measurement of denitrification in a *Prosopis* (mesquite) dominated Sonoran desert ecosystem. Oecologia (Berlin) 53: 120–122.

WEBSTER, R. 1985. Quantitative spatial analysis of soil in the field. Advances in Soil Science 3: 1–70.

WEBSTER, R., AND M. A. OLIVER. 1992. Sample adequately to estimate variograms of soil properties. Journal of Soil Science 43: 177–192.

WEST, N. E. 1981. Nutrient cycling in desert ecosystems. Pages 301–324 *in* D. W. Goodall and R. A. Perry, eds., Arid land ecosystems: structure, function and management. Cambridge University Press, Cambridge, United Kingdom.

_____. 1983. Temperate deserts and semi-deserts: ecosystems of the world. Elsevier Scientific Publishing Co., New York. 522 pp.

WHITFORD, W. G. 1986. Decomposition and nutrient cycling in deserts. Pages 93–117 *in* W. G. Whitford, ed., Patterns and processes in desert ecosystems. University of New Mexico Press, Albuquerque.

ZINKE, P. J. 1962 The pattern of influence of individual forest trees on soil properties. Ecology 43: 130–133.

Received 5 October 1993
Accepted 23 March 1994